

2D SIMULATION OF HIGH-EFFICIENCY CROSS-FIELD RF POWER SOURCES*

Valery A. Dolgashev, Sami G. Tantawi[†], SLAC, Stanford, CA 94309, USA

1 INTRODUCTION

In a cross field device[1] such as magnetron or cross field amplifier electrons move in crossed magnetic and electric fields. Due to synchronism between electron drift velocity and phase velocity of RF wave, the wave bunches the beam, electron spokes are formed and the bunched electrons are decelerated by the RF field. Such devices have high efficiency (up to 90%), high output power and relatively low cost. Electrical design of the cross-field devices is difficult. The problem is 2D (or 3D) and highly nonlinear. It has complex geometry and strong space charge effects. Recently, increased performance of computers and availability of Particle-In-Cell (PIC) codes[2, 3], have made possible the design of relatively low efficiency devices such as relativistic magnetrons or cross field amplifiers [4]. Simulation of high efficiency ($\sim 90\%$) devices is difficult due to the long transient process of starting oscillations. Use of PIC codes for design of such devices is not practical. In this report we describe a frequency domain method that developed for simulating high efficiency cross-field devices. In the method, we consider steady-state interaction of particles with the modes of RF cavity at dominant frequency. Self-consistency of the solution is reached by iterations until power balance is achieved.

2 PHYSICAL MODEL

Cross-field devices consist of a cathode and a surrounding anode. The structure is a cavity with a set of resonant eigenmodes. Macroparticles are emitted from the cathode and moved by forces of electromagnetic fields. The electromagnetic fields are determined by applied external electric potential between anode and cathode, oscillating field of cavity modes, and space charge fields. We use geometry with arbitrary piece-wise planar boundaries. In order to solve the electrostatic and electrodynamic problems, we apply methods that do not require mesh generation. Interaction with magnetic field is determined by uniform magnetic field H_z which is parallel to z -axis and orthogonal to the plane of simulation. There are several assumptions that we use to simplify the problem. These assumptions are based on the working regime of the devices that we want to simulate. Devices will have low current density, are non-relativistic, and have resonant systems with a relatively low density of the cavity modes. Hence, we can neglect magnetic fields due to space charge and cavity modes. We can

also use cavity modes with eigen-frequencies close to the working frequency.

2.1 Basic equations

We are solving a steady state problem of electron beam flow in self-consistent electromagnetic fields. Total fields are superposition of static electric \vec{E}' and magnetic \vec{H}' fields, and “oscillating” electric $\vec{E}(\omega)$ and magnetic $\vec{H}(\omega)$ fields as

$$\vec{E}(t) = \vec{E}' + \Re\{ \vec{E}(\omega)e^{j\omega t} \}, \quad \vec{H}(t) = \vec{H}' + \Re\{ \vec{H}(\omega)e^{j\omega t} \}.$$

Here ω is angular frequency, t is time. We separate the electrodynamic problem into two parts. The first part – electrostatic potential Φ is generated by “external” anode-cathode potential and by the static component of the space-charge electric fields. The second part – the dynamic electromagnetic fields have a harmonic $e^{j\omega t}$ time (t) dependence.

2.2 Static fields

We find the static electric field from $\vec{E}' = -\nabla\Phi$, using the *Poisson equation*:

$$\nabla^2\Phi = -\frac{\rho}{\epsilon_0}, \quad (1)$$

where ∇ is the gradient operator, ρ is volume charge density averaged over oscillation period $T = 2\pi/\omega$. ϵ_0 is the electric permittivity of the vacuum.

2.3 Oscillating fields

To solve the second part of the problem, we write the time harmonic *Maxwell equations* as

$$\nabla \times \vec{E} = -j\omega\mu_0\vec{H}, \quad \nabla \times \vec{H} = j\omega\epsilon_0\vec{E} + \vec{J}_\omega. \quad (2)$$

Here \vec{J}_ω is electric current density, μ_0 is the magnetic permeability of vacuum. Oscillating fields inside a cavity are expanded in terms of the cavity eigenmodes (\vec{E}_s, \vec{H}_s) and the *fast oscillating* electric potential φ_ω as

$$\vec{E} = \sum_s A_s \vec{E}_s - \nabla\varphi_\omega, \quad \vec{H} = \sum_s B_s \vec{H}_s. \quad (3)$$

Here s is mode index, A_s and B_s are the eigenmode amplitudes. Using the expansion (3) we get the *Poisson equation* for the potential:

$$\nabla^2\varphi = \frac{\nabla \cdot \vec{J}_\omega}{j\omega\epsilon_0} = -\frac{\rho_\omega}{\epsilon_0}, \quad (4)$$

where ρ_ω is the oscillating space-charge density. Amplitudes of the electric field expansion are given by

$$A_s = \frac{\omega}{j(\omega^2 - \omega_s^2)} \frac{\int_V \vec{J}_\omega \cdot \vec{E}_s^* dV}{\epsilon_0 \int_V \vec{E}_s \cdot \vec{E}_s^* dV}. \quad (5)$$

Here ω_s is the mode eigen-frequency of the mode, V is the cavity volume.

* This work was supported by the U.S. Department of Energy contract DE-AC03-76SF00515.

[†] Also with the Communications and Electronics Department, Cairo University, Giza, Egypt.

2.4 Equation of motion

Equation of motion for an electron in crossed-fields is

$$\frac{d\vec{p}}{dt} = q_e \vec{E}(t) + \mu_0 \vec{v} \times H_z, \quad (6)$$

where \vec{p} is the relativistic momentum, q_e is the charge, and \vec{v} is the velocity of the electron. Current density induced by the electron motion is $\vec{J} = q_e \vec{v} \delta(\vec{r})$, where \vec{r} is the position vector of the electron, and δ is the *Kronecker delta function*.

3 NUMERICAL METHODS

We created several separate program modules to simulate a cross-field device. First is an *RF field solver* that calculates eigenmodes and eigen-frequencies in the cavity; second is the *Poisson solver* that finds electric fields due to external potential, static space charge, and oscillating space charge; and third, the *tracking module* that performs tracking of electrons through electromagnetic fields. For simulation, we consider an arbitrary, piecewise bounded 2D geometry.

3.1 Planar geometry

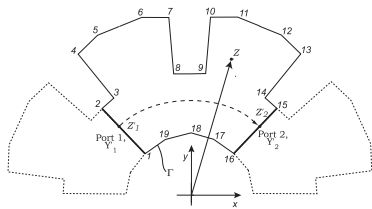


Figure 1: Planar geometry.

The geometry is cylindrical (uniform in the z -direction) as illustrated on Fig. 1. It consists of planar sidewalls and apertures. The geometry in the x, y plane can be described by a set of points $z_s = (x_s, y_s)$, where $s = 1, 2, \dots, N'$; here N' is the total number of sidewalls and apertures. Periodic boundary conditions are applied to the apertures. The periodic boundary allows us to use only part of the structure and significantly reduce simulation time. In the particular case shown in Fig. 1 the geometry has $N' = 19$ sidewalls, two apertures (ports) with starting points $p = 1, 15$, and the cathode and anode determined by $s = 16, 17, 18, 19, 1$ and $s = 2, 3, \dots, 15$ respectively.

3.2 RF field solver

The description of the RF solver that is used in this method is published in [5]. Here we briefly outline its properties. We use the scattering matrix approach [6] to calculate the dispersion parameters of the periodic 2D structure, its resonant frequencies, and the corresponding fields. The fields are described by functional expansion. Boundary contour mode-matching is applied in a piecewise bounded 2D region is applied to obtain the scattering matrix and field amplitudes [7]. The Galerkin method is used for the mode-matching procedure. The geometry is divided into regions, and electromagnetic fields in each region are expanded in

series of plane waves or (for low frequencies) *Bessel functions*. Scattering matrices from the regions are combined using the generalized scattering matrix technique. Resonant and periodic boundary conditions [6] are used to obtain resonant frequencies, dispersion parameters, and corresponding fields. We calculate the electric fields on a polar grid (only in the region of field-particle interaction), in order to speed up calculation of fields for the macroparticle tracking. To obtain field at the macroparticle position we use 2D spline interpolation.

3.3 Poisson solver

We use an efficient method for solving the Poisson equation for electric fields in a 2-D, arbitrarily shaped geometry. The solution is based on the method of moments. Point-matching in a piecewise bounded 2D region is applied to obtain the charge density on the boundary. The boundary's charge density determines the fields and potentials throughout the interior region. We use a complex representation of the fields and potentials in the solution [8]. We apply periodic boundary conditions to simulate the fields in the periodic structure.

Formulation We solve equation (1) in 2D. In the 2D case it is advantageous to represent the position and field vector's (x, y) components by a single complex representation. We will work with functions of a complex variable $z = x + jy$. The field strength \vec{E} can be written in terms of the scalar potential $\Phi = \Phi(z)$ as

$$\vec{E}(z) = -\frac{d\Phi^*}{dz}. \quad (7)$$

Here $*$ represents the complex conjugate. An effective line charge q (point charge in 2D geometry) has the complex potential $\Phi = (q/\epsilon_0) \log z$. We approximate the charge distribution on the boundary of the region as a sum of "step" functions. We divide each element (sidewall and aperture) of the boundary into N_b straight pieces or "charged lines" with uniform charge density σ along the piece. A *uniformly charged straight wall* with beginning and end coordinates z_1 and z_2 , respectively, will produce a complex potential at the point z_w

$$\Phi(z_w) = \int_L \frac{\sigma}{\epsilon_0} \log(z - z_w) dz, \quad (8)$$

where L is the contour along the line. Equation (8) is integrated analytically.

Field strength of the charged wall We obtain the electric field of the *charged line* by substituting (8) into (7):

$$\frac{\vec{E}(z_w)\epsilon_0}{\sigma} = \left[\frac{|z_1 - z_2|}{z_1 - z_2} \log \left(\frac{z_w - z_1}{z_w - z_2} \right) \right]^*. \quad (9)$$

The value of the function is undefined on the line's contour. However, for us, the fields inside the region are of interest. Therefore, the direction of the field (for positive charge)

on the line's contour is chosen to be directed inward. Also singularities at points z_1 and z_2 can affect the field's calculation. Macroparticles with finite dimensions are used to avoid this singularity.

Periodic boundary condition We assume that the potential and field strength are repeated on the period's apertures (Fig. 1). Let $z'_1 \in Y'_1$ and $z'_2 \in Y'_2$. If we shift the region to the right so it coincides with the next period, the coordinate z'_1 will be transformed into coordinate z'_2 . The periodic boundary condition becomes

$$\Phi(z'_1) = \Phi(z'_2), \quad \frac{\partial \Phi(z'_1)}{\partial n} = -\frac{\partial \Phi(z'_2)}{\partial n}. \quad (10)$$

We assume the Dirichlet condition on the sidewalls (except for the apertures) as

$$\Phi(\Gamma') = \zeta(\Gamma'), \quad \Gamma = \Gamma' + Y'_1 + Y'_2. \quad (11)$$

Integral equations For periodic boundary conditions (10) and (11) surface charge density σ must satisfy the coupled integral equations

$$\left\{ \begin{array}{l} \int_{\Gamma} \log(z_w - z) \sigma(z) dz = \epsilon_0 \zeta(z_w), \quad z_w \in \Gamma', \\ \int_{\Gamma} \log(z'_1 - z) \sigma(z) dz = \int_{\Gamma} \log(z'_2 - z) \sigma(z) dz, \\ \int_{\Gamma} \left\{ \frac{\partial \log(z'_1 - z)}{\partial n_p} \right\}^* \sigma(z) dz + \pi \sigma(z'_1) = \\ = - \int_{\Gamma} \left\{ \frac{\partial \log(z'_2 - z)}{\partial n_p} \right\}^* \sigma(z) dz - \pi \sigma(z_2), \\ z \in \Gamma, z'_1 \in Y'_1, z'_2 \in Y'_2, \end{array} \right\}, \quad (12)$$

in which $\frac{\partial \log(z_w - z)}{\partial n_p}$ denotes the normal derivative of $\log(z_w - z)$ at the point z_w assuming z is fixed; $\Gamma = \Gamma' + Y'_1 + Y'_2$; coordinates z_1 and z_2 are the same as in (10); and $\zeta(z_w)$ is the external potential.

Numerical approximation We solve the integral equation numerically, by approximating the source densities by step-functions [9]. Thus we divide the given boundary Γ into N_{Γ} intervals and assume that the simple source density σ has a constant value within each interval. Then denoting these constant values by σ_i , $i = 1, 2, \dots, N_{\Gamma}$, we approximate Φ and E by

$$\hat{\Phi}(z_w) = \sum_{i=1}^{N_{\Gamma}} \sigma_i \epsilon_0 \int_i \log(z_w - z) dz, \quad \text{and} \quad (13)$$

$$\hat{E}(z_w) = \sum_{i=1}^{N_{\Gamma}} \frac{\sigma_i}{\epsilon_0} \int_i \left(\frac{d \log(z_w - z)}{dz_w} \right)^* dz, \quad (14)$$

where \int_i denotes integration over the i -th interval of Γ . We substitute (13) and (14) into (12) to obtain numerical approximation for periodic solution. The unknowns (in the system obtained) are the charge density on the intervals σ_i , the potential and the electric field on the periodic aperture. All coefficients in the system are calculated analytically. For practical geometries, the matrix of coefficients is well

defined and there is no difficulty in solving the system directly. For macroparticle tracking, the electric field calculated on polar grid and then interpolated at the macroparticle position (same as for RF fields).

3.4 Tracking

We find a macroparticle trajectory by using the 4th order Runge-Kutta method for integrating the equation of motion (6) in polar coordinates. Then, we integrate the complex electric field of the cavity modes along the trajectory to find coefficients for the cavity's eigenmodes (5). We monitor energy conservation in order to verify accuracy of calculation. For that purpose we use total energy that consists of kinetic energy of the macroparticle and integral of static (due to external potential and static space charge) and oscillating (due to cavity modes and oscillating space charge) electric fields along the trajectory. Initial charge and velocity \vec{v} are determined by a space-charge-limited-emission model and a relaxation scheme.

3.5 Algorithm

We start simulation by calculating dispersion the curve for the spatial period of the device (using the *RF field solver*). Then, we calculate electric fields for the eigenmodes. Next, (using the *Poisson solver*) we calculate electric field due to external potential. Next, we start iterations using *Tracking module* to find the macroparticle trajectories, field integrals along the trajectories, and electric fields due to space charge. Next, we update the static and oscillating fields and start new iteration.

4 SUMMARY

We have written a C++ computer code that uses methods, described above. Accuracy of resonant frequency calculation by *RF field solver* for typical geometries is $\sim 0.1\%$. We tested performance of *Poisson solver* and *Tracking module* on diode geometries (without magnetic field). We calculated diode current with typical accuracy 2-3% in comparison with analytical solution. Testing of the code on cross-field devices is under way.

5 REFERENCES

- [1] G. B. Collins, "Microwave Magnetrons," Boston tech. pub., Inc., 1964.
- [2] B. Goplen *et al*, "User-configurable MAGIC Code for Electromagnetic PIC Calculations," *Comp. Phys. Comm.*, vol.87, pp. 54-86, 1995.
- [3] K. R. Eppley, "Numerical Simulation Of Cross Field Amplifiers," SLAC-PUB-5183, 1990.
- [4] X. Chen, *et al*, "2D/3D magnetron modeling," *2nd Int. Conf. On Cross Field Devices and Appl.*, Boston, MA, USA, 17-19 June, 1998.
- [5] V.A. Dolgashev, S.G. Tantawi, "Method for Efficient Analysis of Waveguide Components and Cavities for RF Sources," EPAC'2000, 26-30 June 2000, Austria Center, Vienna.
- [6] V. A. Dolgashev, "Calculation of Impedance for Multiple Waveguide Junction Using Scattering Matrix Formulation," presented at ICAP'98, Monterrey, CA, USA, 14-18 Sept., 1998.
- [7] J. M. Reiter and F. Arndt, *IEEE Trans. Microwave Theory Tech.*, vol. 43, pp. 796-801, Apr. 1995.
- [8] R. B. Beth, "Complex Representation and Computation of Two-Dimensional Magnetic Fields", *Journal of Applied Physics*, Vol. 37, Number 7, June, 1966.
- [9] L. M. Delves and J. Walsh, "Numerical Solution of Integral Equations," Clarendon Press, Oxford, 1974.